SOURCE SIZE EFFECTS ON CAVITATION DAMAGE

M. A. Hosien [†] and S. M. Selim

Mechanical Power Engineering Department, Faculty of Engineering, Menoufyia University, Shebin El-Kom, Egypt

†Corresponding Author Email: mohamed_abdelaziz14@ yahoo.com

ABSTRACT

Cavitation is important as a consequence of its effects. Uncontrolled cavitation can produce serious erosion to all materials. In the light of the current world wide interest in the problem of cavitation damage prediction and scaling, it was decided to evaluate the effects of source size on the cavitation damage. For this purpose, an experimental study of the effect of source size on the weight loss rate in the steady–state zone of pure aluminum test specimens was conducted using three different shapes of cavitation inducer to represent the types of cavitation normally occur in practice. For each source shape seven sizes from 15 mm to 27 mm were used. The tests were performed in two separate groups, one at constant cavitation number and various flow velocities (24-42.5 m/s) and the other at constant flow velocity and different cavitation numbers (0.017-0.15)for each source size.

The results showed that, for all flow conditions and source shapes and sizes, the weight loss rate (WLR) increased up to blockage ratio (B) of about 0.5 and then decreased with increasing blockage ratio. Also the results indicated that the weight loss rate was proportional to the source size raised to two characteristic powers: $\propto D^{e_1}$, ($0.353 \ll B \ll 0.47$) , with positive index (e_1) and WLR $\propto D^{e_2}$, ($0.47 \ll B \ll 0.635$) , with negative index (e_2). The values of e_1 and e_2 were varied quite widely depending on the flow conditions, source shape and size and place of erosion. The magnitudes of e_1 and e_2 were varied from 1.88 to 5.09 and from -1.92 to -11.3, respectively. In addition, the results illustrated that the size exponent's e_1 and e_2 were varied approximately exponentially with both the flow velocity and cavitation number. The values of flow velocity and cavitation number exponents were varied widely between cavitation source shape and place of erosion measurements.

The results presented herein have proved that the effect of source size on cavitation damage is extremely complex and no general scaling laws can be established at present. Undoubtedly, further systematic studies should be carried out.

Keywords: Cavitation; Erosion; Velocity exponent; Source size; Weight loss rate.

اثار حجم المصدر على ضرر التكهف

التكهف مهم نتيجة لآثاره . . يمكن أن يؤدي التكهف غير المنضبط إلى تآكل خطير لجميع المواد. في ضوء الاهتمام العالمي الحالي في مشكلة التنبؤ بضرر التكهف والتوسع تقرر تقييم آثار حجم المصدر على ضرر التكهف. لهذا الغرض، أجريت دراسة تجريبية لتأثير حجم المصدر على معدل فقدان الوزن في منطقة ثابتة من عينات اختبار الألومنيوم النقي باستخدام ثلاثة أشكال مختلفة من محفز التكهف لتمثيل أنواع التكهف التى تحدث عادة في الممارسة العملية. لكل شكل مصدر استخدمت سبعة أحجام من 15 ملم إلى 27 ملم. أجريت الاختبارات في مجموعتين منفصلتين، واحدة عند ثبوت معامل التكهف وسرعات تدفق مختلفة (24-42.5 م / ث) والآخر في سرعة تدفق ثابتة ومعاملات تكهف مختلفة (0.017-0.15) لكل حجم مصدر.

وأظهرت النتائج أنه بالنسبة لجميع ظروف التدفق وأشكال وأحجام المصدر، زاد معدل فقدان الوزن (WLR) حتى نسبة الانسداد (B) حوالي 0.5 ثم انخفض مع زيادة نسبة الانسداد. كما أشارت النتائج إلى أن معدل فقدان الوزن كان متناسبا مع حجم المصدر الذي تم رفعه إلى اسين مميزتين∝ D^{e_1} , ($0.353 \ll B \ll 0.47$) و (e₁) واس موجب و WLR ∝ D^{e_2} , ($0.47 \ll B \ll 0.635$) واس سالب (e₂). . كانت قيم e_1 و e_2 متنوعة فى نطاق واسع اعتمادا على ظروف التدفق، شكل المصدر وحجم ومكان التأكل. وتراوحت قيم e_1 و e_2 من 1.88 الى 5.09 ومن -1.92 الى -11.3 على التوالى . . وبالإضافة إلى ذلك، أظهرت النتائج أن اس حجم المصدر e_1 و e_2 تتغير بشكل أسي مع كل من سرعة التدفق ومعامل التكهف. وتفاوتت قيم اس سرعة التدفق ومعامل التكهف فى نطاق واسع بين شكل مصدر التكهف ومكان قياسات التآكل.

وقد أثبتت النتائج الواردة في هذا البحث أن تأثير حجم المصدر على ضرر التكهف معقدة للغاية ولا يمكن وضع قوانين عامة للقياس في الوقت الحاضر. ومما لا شك فيه أنه ينبغي إجراء مزيد من الدراسات المنهجية.

1. INTRODUCTION

The study of the cavitation erosion in fluid flow has formed the subject of numerous publications during this century. The existence of cavitation in flowing system can produce serious erosion damage to all materials. Although the literature provides a good guide to the erosion resistance of various materials and how erosion damage initiation and progress, the ability to predict cavitation erosion rates in prototype hydraulic machines operating at various conditions from model tests still far from complete. It is evident that accurate information of the influence of size on the amount of erosion likely at different operating conditions is very important for the design engineers to assess erosion rate for full size machine from tests on model. Only very few investigators realized the importance of the influence of size on erosion.

Size scaling in cavitation erosion is a major problem confronting the design engineers of modern high speed machinery.

Rao and Buckley [1] presented an overview study and erosion data analysis which indicated that the size scale exponent n in the relation erosion rate α (size or diameter)^n can vary from 1.7 to 4.9 depending on the type of device used. There is, however, a general agreement as to the values of n if the correlations are made with constant cavitation number.

Ramamurthy *et al.* [2] conducted cavitation damage tests in a rotating disk facility by varying the source size, the source velocity and the chamber pressure. Two dimensional triangular prismatic shapes were used as cavitating sources to reduce the significance of Reynolds number in interpreting the test results. The results indicate that the velocity exponent at maximum cavitation damage conditions is 5.95 and that maximum damage occurs in a narrow band of cavitation numbers. The results also indicate that the critical size of the source for maximum erosion increases with cavitation number.

Ramamurthy and Bhaskaran [3] conducted tests in a rotating disk facility to determine the effects of source size and velocity on cavitation damage in aluminum test specimens. To eliminate Reynolds number as a primary parameter, the shape of the cavitating source was chosen to be triangular. For a given relative velocity of the flow, there is an optimum size of the source for which the damage in the specimen is a maximum.

Previous researches [4-29] showed that the cavitating source size play an important factor in the cavitation erosion rate .The effect of size on the cavitation erosion rate has been commonly expressed by an exponential dependence of source size. The size exponents reported by various investigators are presented in Table A1 (shown in appendix A). From this table it is apparent that the size exponent (e) values are in the range 2.2 to 8.4 depending on the test devices, conditions, materials and the erosion stage. Although the tests of various investigators in Table A1 supported the exponential dependence of source size, it is not possible to obtain reliable information or size scale effects. This is perhaps the cavitation erosion process involves with conditions which were too complex. Accordingly, systematic reliable erosion experiments and analysis are required to understand the size effects on cavitation erosion rate at various flow conditions and different types of cavitation normally encountered in practice and to realize the limitations of the present knowledge. Therefore, the present work set out to provide reliable experimental data in the cavitating source size effects on erosion rate at various flow conditions and different source geometries to simulate the types of cavitation occur in practice.

2. EXPERIMENTAL TECHNIQUE
2.1 Test Equipment
For the experimental work a two-dimensional closed circuit water tunnel at Menoufiya University was used because it offered conditions which were reasonably similar to prototype flow conditions. A new working section of 42.5x18.5 mm cross-sectional was made from 20 mm thick iron to resist the stresses resulting from bubble collapse. Two transparent Perspex windows were machined to engage into the windows of the two smaller sides of the working section, and were backed up by a two iron windows. This is to observe the cavity during the operation of the tunnel for long period and to keep the operation condition constant.

In order to replenish the water loss from the rig through the pump sealing glands a high pressure supply system was added to the test rig. This is to keep the circuit operating long time at fairly constant pressure during the test.

It was noticed that when the tunnel operates for long period, the temperature of working water increases rapidly. For this reason a new cooling system was designed and fitted to operate the tunnel for long time at constant desired temperature.

A detailed description of the water tunnel is available elsewhere, Hosien and Selim [30 and 31].

2.2 Cavitation Source Configurations
The experiments described here were done using three different configurations for inducing cavitation. The flow in such configurations is relevant to many practical situations such as hydraulic machines. These configurations were 60^0 symmetrical wedge, circular cylinder and convergent – divergent wedge. The three different configurations were selected to represent the types of cavitation normally occur in practice. The 60^0 symmetric wedges represent the type of vortex cavitation which occurs in the cores of vortices behind the source. The circular cylinder represents the travelling cavitation appears along the surface and grows in the wake zone of the cylinder. The convergent-divergent wedge represents the cyclic fixed cavity attached to the solid boundary of the cavitation source.

Fig. 1 shows the cavitation sources and their position in the working section along with erosion test specimens. For each source configuration seven sizes of 15, 17, 18.5, 20, 22, 24 and 26 mm (note: the biggest size for 60^0 symmetrical wedges is 27 mm instead off 26 mm) with 18.5 mm height were used.
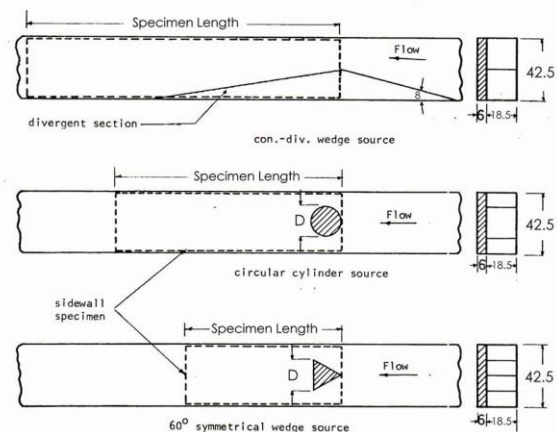

Fig.1. Cavitation source configurations. (Dim. in mm)

2.3 Erosion Test Specimens

The material used for all erosion test specimens was 99.0% pure aluminum (SIC, B.S.1470), fabricated and no heat treatment because it would suitable for use in erosion research. All specimens were taken from the same plate or rod in order to keep the same material specifications for all tests. The specimen shapes were used a plate of 160 mm length, 42.5 mm width and 6 mm thickness and a cylindrical of different diameters and 18.5 mm height. The erosion specimen was flushing mounted in the cover of the working section of the water tunnel underneath the source and extended downstream the source.

The specimens were polished with a fine grade silicon paper carbide paper and its roughness value (CLA) was of order 10 μm.

2.4 Test Conditions

The velocity, the pressure and duration of the erosion test were varied for each cavitation source while all other parameters were holding constant. The velocity was varied from 24 m/s to 40 m/s at a constant cavitation number of 0.035 for circular cylinder and con. – div. wedge cavitation source sizes. The velocity was varied from 24 to 42.5 m/s at a constant cavitation number of 0.113 for 60^0 symmetric wedge sources. The cavitation number was varied from 0.06 to 0.138 at 37.6 m/s for 60^0 symmetric wedge sources, 0.013 to 0.15 at 37 m/s for circular cylinder sources, and 0.01 to 0.075 at 37 m/s for the con. – div. wedge sources.

The tunnel water temperature of 32 ± 2 ^{o}c was kept fairly constant by regulating the amount of cooling water flowing through the cooling coils and it was noted repeatedly during the tests.

2.5 Test Procedure and Preliminary Tests

Prior to the tests, the tunnel was run under intense cavitating conditions for ten minutes and air from water bled off to achieve equilibrium air content before conducting erosion tests.

The specimen was initially weighed with the help of a precision electronic balance, Oertling LA 264, whose lowest count was 0.l mg. It was mounted in the cover of the test section. For weight loss tests, the flow pressure was raised to the point where the desired cavitation condition would occur. Then the specimen exposed to the required cavitation attack condition for a desired length of time which depends on the intensity of the cavitation attack, after which it was removed from the cover of the water tunnel and reweighed. Before each weighing the specimen was cleaned and dried.

For weight-loss/time studies the specimen was repeatedly subjected to cavitation attack for definite intervals of time until satisfactory points in the steady-state weight loss zone have been obtained. The weight loss rate (WLR) can be obtained from the weight loss versus exposure time curve, i.e., the slope of the steady –state zone. The unit of the weight loss rate is mg/hr.

Preliminary tests were conducted before conducting the actual erosion tests. The tests were performed for the three configurations to: (i) determine the maximum and minimum cavitation numbers and flow velocities, (ii) choose a suitable sidewall specimens length at minimum cavitation number, (iii) find a suitable weight loss time measurement increment, and (iv) evaluate the repeatability of weight loss measurement at the same flow condition and fixed duration for all configurations.

The results of these tests indicated that both weight loss and the side wall specimen's length varied widely with the shape of the configuration.

The weight loss produced by the 60^0 symmetrical wedges was more severe than that for the circular cylinder and the con.-div. wedge. This is due to the variation in the cavitation intensity with the shape of cavitation sources. Therefore, the weight loss time measurement increment varied with each configuration. In addition the variation in lengths of the sidewall specimens with the shape of the cavitation sources was due to the different in the maximum lengths required for weight loss area at minimum cavitation number.

2. 6 Measurements Error and Repeatability

A pressure transducer of model Phillips order no.9880/20 was used to measure the inlet pressure of the test section. This pressure is used to calculate the cavitation number. The accuracy of the pressure measurement was about ± 0.4%. The velocity of the flow in the working section was obtained from the output signal of an electromagnetic flow meter. The accuracy of velocity was about ± 0.5%.

A precise digital stopwatch is used for the measurement of the test duration was started after stable conditions were reached.

A thermometer is used to measure the temperature of water in the tunnel with accuracy of ± 1.5 ^{o}C. This means that the uncertainty of vapour pressure is insignificant. Therefore, the extreme error in cavitation number is 1.8% for higher cavitation numbers and 4% for lower cavitation numbers. The accuracy of weight loss, particularly in the steady-state weight loss zone was within ±0.5%. Considering the error in the operation conditions, it appears that the weight loss results are accurate to within ± 4.5%.

The normal statistical analysis of repeatability weight loss tests of fifteen sidewall specimens for the three configurations yielded that the 95 percent confidence limits of weight loss measurements at 3 hours duration for the three configurations were 1.6 %, 2.2 %, and 3.25% for 60^0 symmetrical wedge, circular cylinder, and con.-div. cavitation sources, respectively.

3. EXPERIMENTAL RESULS AND DISCUSSION

Extensive experiments were conducted at a wide range of velocities (24 m/s to 42.5 m/s), cavitation numbers (0.01 to 0.15) and seven sizes (15-27mm) for the three configurations to demonstrate the effect of source size on weight loss rate (WLR). The portions of the weight loss rate versus time curves which are of constant slope were taken to be the weight loss rate (WLR) for respective test conditions. In order to establish the size scale effect on the WLR the results were plotted on a double logarithmic scale in Figs. 2 to 9. These Figures summarize the results of the extensive experiments. The results indicate that in all tests the eight loss rate (WLR) depends strongly on the size of cavitation source. Moreover, the results illustrate that the weight loss rate increases with increasing the cavitating source size up to a certain source size (D) or blockage ratio(B), reaches a maximum and then decreases with increasing the source size.
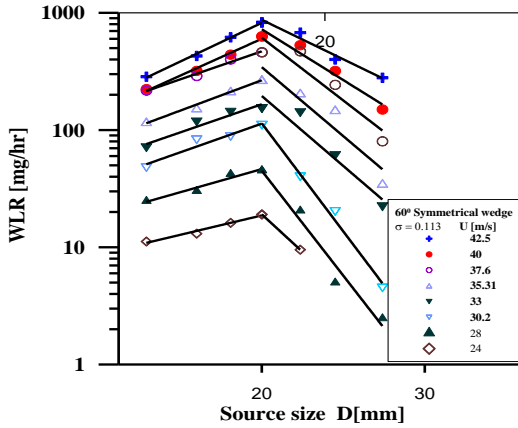
Fig. 2. Effect of source size on weight loss rate for 60⁰ symmetrical wedge side wall erosion at various flow velocities and constant cavitation number of 0.113.
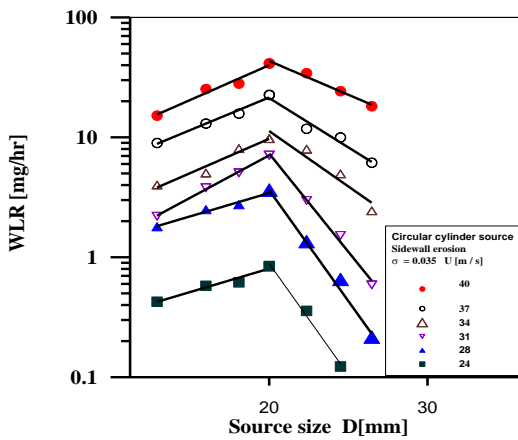

Fig. 3. Effect of source size on weight loss rate for circular cylinder source side wall erosion at various flow velocities with constant flow cavitation number of .035.
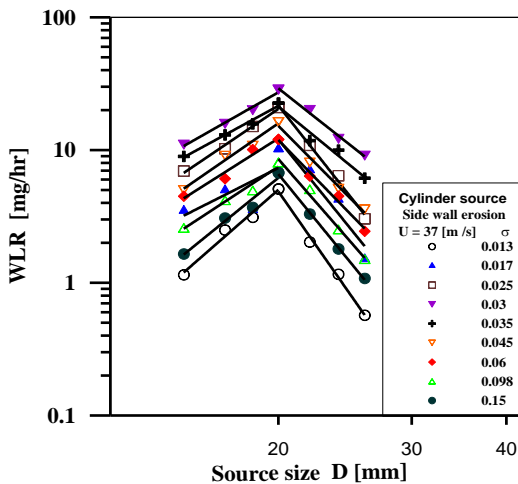

Fig. 4. Effect of source size on weight loss rate for circular cylinder side wall erosion at various cavitation numbers with constant flow velocity of 37 m/s.
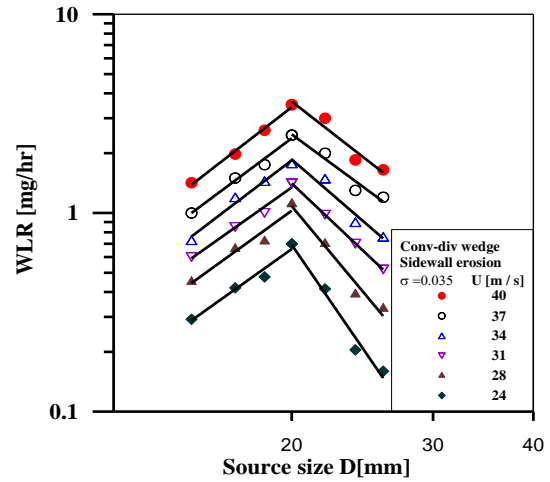

Fig. 5. Effect of source size on weight loss rate for con.-div. wedge side wall erosion and various flow velocities and constant cavitation number of 0.035.
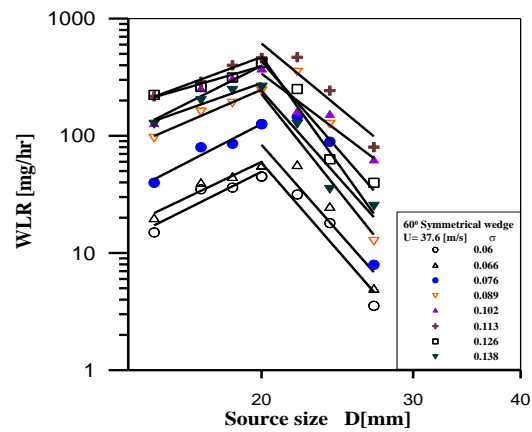

Fig. 6. Effect of source size on weight loss rate for 60⁰ symmetrical wedges at various cavitation numbers with constant flow velocity of 37.6 m/s.
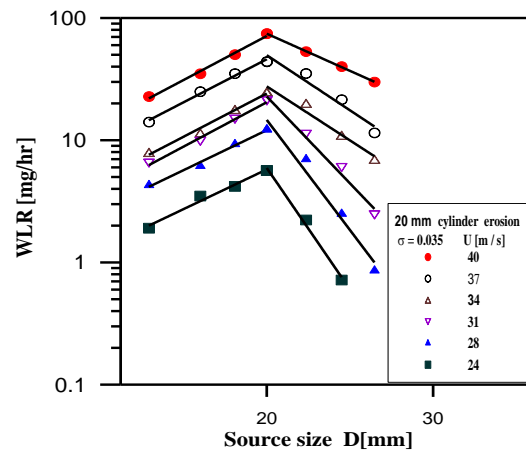

Fig. 7. Effect of source size on weight loss rate for circular cylinder erosion and various flow velocities with constant cavitation number of 0.035.
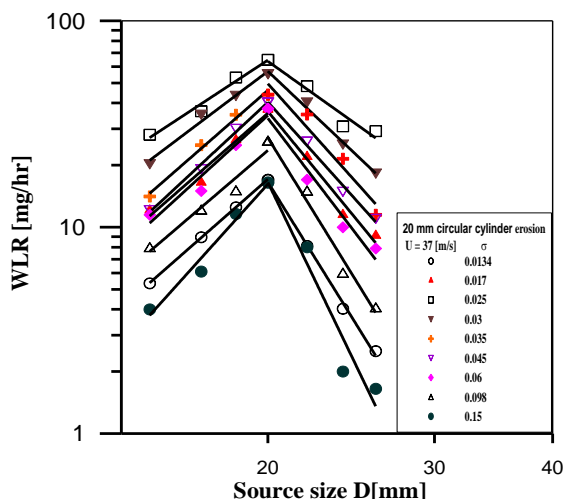
Fig. 8. Effect of source size on weight loss rate for circular cylinder erosion at various cavitation numbers with constant velocity of 37 m/s.
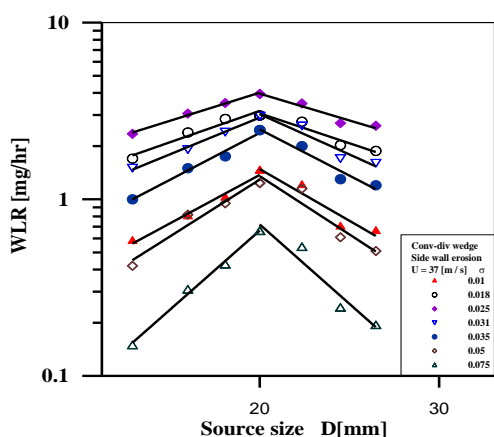

Fig. 9. Effect of source size on weight loss rate for con.-div. wedge side wall erosion at various cavitation number

In general Figures 2 to 9 show that (WLR) is proportional to the source size raised to two characteristic powers: WLR $\propto$ D^{e_1} and WLR $\propto D^{e_2}$ one is positive in the size range of 15 mm $(B = 0.353)$ to 20 mm $(B = 0.47)$ and the second is negative in the size range of 20 mm $(B = 0.47)$ to 27 mm $(B = 0.635)$. The size exponents (e_1, e_2) for all tests are presented in Table A2.

The exact variations of WLR with size at constant cavitation number with various flow velocities for the three configurations are shown in Figures 2 to 5. These Figures show that at larger velocity the variation of WLR with size was larger and the maximum weight loss rate (WLR$_{max}$) was larger. The maximum weight loss rate for all tests occurs at blockage ratio, *B*, of about 0.47.

Figures 6 to 9 show the variation of WLR with source size at constant flow velocity with various cavitation numbers. These Figures indicate similar trend of the variation of WLR with size at constant cavitation number with various velocities which are shown in Figs. 2 to 5. In addition Figs 6 to 9 indicate that the variation of WLR with size at the intermediate values of cavitation numbers is larger than that at higher or lower values of cavitation numbers.

The variation of the weight loss rate with cavitation source size can be attributing to the following. As the cavitation source size is increased at conditions of constant cavitation regime, more bubbles are produced from the spectrum of the free stream nuclei and swept into the collapse zone resulting in an increase of the overall collapsing energy of the bubbles. Since an increase of cavitation source size will increase the average bubble size due to the increase in the area available for bubble growth (longer cavity length). Therefore the damage potential of the larger bubble sizes are higher since the duration of the impacting microjet produced from the collapsing bubble is longer. Moreover, changing the source size affects the collapse driving pressure (the difference of pressure between the outside and inside of the bubble), standoff distance (distance between the initial bubble center location and the rigid surface) and the thin water layer between the collapse bubble surface and the rigid boundary. The speed of the bubble collapse and the impact efficiency depends on the pressure driving collapse. As the driving pressure increases the velocity of the jet increases with square root of the driving pressure, the characteristic time of the bubble during collapse decreases, and improves the impact efficiency. These factors produce a strong jet with large impact energy. As the standoff distance decreases the bubble collapse period increases causing an increase in the terminal velocity of the jet as well documented in the literature [5, 22, 23 and 24]. The results in an increase in the impact pressure reported in [25, 26, 27, 28 and 29].

Consequently, the expected weight loss rate increases up to a particular cavitation source size and then starts to decrease. A further increase in the cavitation source size increases the frequency of pressure fluctuations. Thus the number of bubbles decreases resulting in lower bubble collapse energy. This is reflected in the increased weight loss rate up to a certain limiting cavitation source size. In other words, for a given set of controlled cavitation conditions (fixed velocity and cavitation number), there is a combined effect of cavitation source size and frequency of pressure pulsations which render the weight loss rete to be a maximum. Clearly, when the source size is made extremely small its effect is local and no serious cavitation damage should be expected. In addition, it was noticed that : (1) during the operation of the test rig,, the separation zone increases downstream with increasing the cavitation source in size, (2) by using the 26 mm source size, at the moment of shut-off the rig, it was observed a number of bubbles with larger volume behind the source than that for other sizes used, (3) with larger sizes the cavity length was larger than the other sizes, and not well-defined contour as at smaller size; and the emission noise, due to cavitation, was lower in comparison to other sizes. The erosion area was larger for the larger values of source sizes, results in a lower weight loss rate due to the collapse energy being distributed over a larger area, and (4) The interaction between the boundary layer thickness at the test section wall and the cavity boundary alters the local pressure distribution along the cavity boundary, the cavity geometry and the speed of sound and liquid density. This leads to a decrease in the number of collapsing bubbles and their average size resulting in lower collapse energy.

Therefore, the following factors may play a role for the reduction in weight loss rate at larger cavitation source sizes (i.e., smaller clearance or higher blockage ratio): 1. insufficient momentum of re-entrant jet motion to reach the trailing edge of the cavity, leaving the upstream portion of

the cavity steady. Thus the bubbles cluster volume produced by re-entrant jet after break off is smaller, resulting in less collapsing energy, 2. a lower collapse pressure due to the fluctuations of the cavity length along the surface of specimen, 3. reduction in the number of collapsing cavities resulting in less collapsing energy. This is due to increasing the pressure level in the test section with source size which tends to reduce both the average size and the growth time of the nuclei, and 4. decrease in the volume of the collapsing cavity.

In order to establish the relation between weight loss rate and cavitation source size, the experimental results are plotted on a double logarithmic scale in Figures 2 to 9. The best fit straight lines to the results are estimated using least squares. The slopes of the lines are taken to be the exponents of the cavitation source size, e_1 and e_2 for respective cavitation source shape and test conditions. The size exponents derived from Figures 2 to 9 are presented in Table A2 (shown in appendix A). Table A2 includes the correlation coefficients. The experimental results corresponding to a particular cavitation source were analyzed in two separate groups, one at constant flow velocity and various cavitation numbers and the others at constant cavitation number with different flow velocities. In comparing the experimental values of the size exponents (e_1 and e_2), Table A2, it can see that their magnitudes are different and depend on many factors such as cavitation source shape, place of weight loss measurement , and test condition i.e., constant flow velocity or constant cavitation number. An examination of e_1 and e_2 magnitudes indicates that e_1 various between 1.88 and 5.09 and e_2 can lie anywhere between -1.92 and -11.3.This wide variation in the magnitudes of e_1 and e_2 provides an insight into the disagreements in the published results related to the size exponent as listed in Table A1. In general the accepted belief is that there is no general size exponent.

This particular aspect of size exponents reported in the present investigation has not been widely reported in earlier investigations.

The difference in the magnitudes of size exponents reported herein may be attributed to the following: (i) change in the type of cavitation as each cavitation source shape produced different dynamic structure and classes of cavitation; (ii) the pressure gradient in the test section is a function of the shape of the cavitation source. Therefore every source shape will exhibit different flow regime, cavity shape and length, frequency of cavity cycle; (iii) values of incipient and breakdown cavitation numbers are function of cavitation source shape and size; (iv) mechanism of bubbles collapse and erosion is quite different for each cavitation source shape.

The effects on source size exponents (e_1 and e_2) of changing either constant cavitation number and variable flow velocity or vice-versa are shown in Figures 10 to 13.
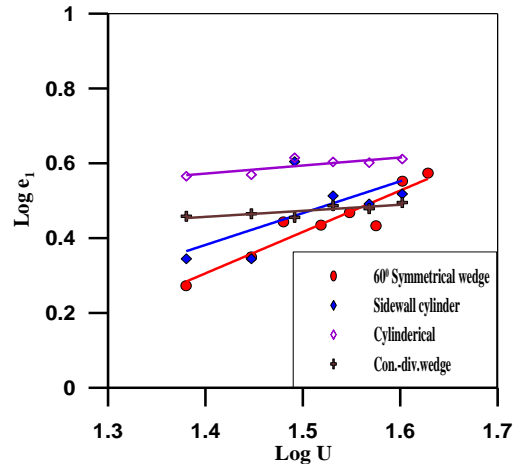

Fig.10. Variation of size exponent e_1 with flow velocity at constant   cavitation numbers for various sources.
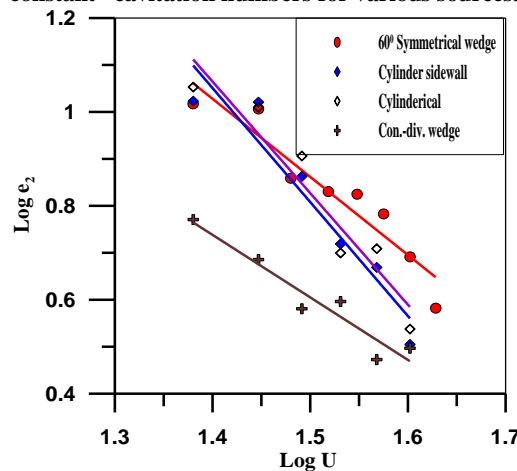

Fig.11. Variation of size exponent e_2 with flow velocity at constant   cavitation numbers for various sources.
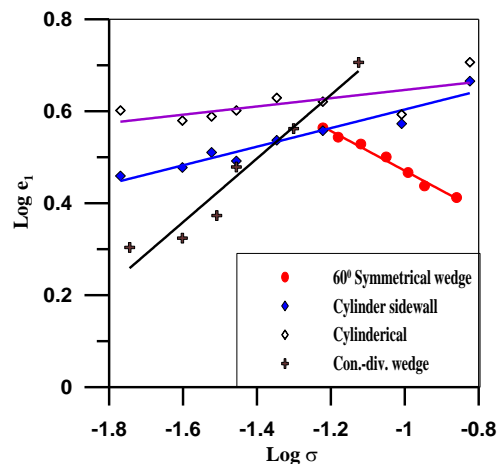

Fig.12. Variation of size exponent e_1 with cavitation number at various flow velocities for various sources.
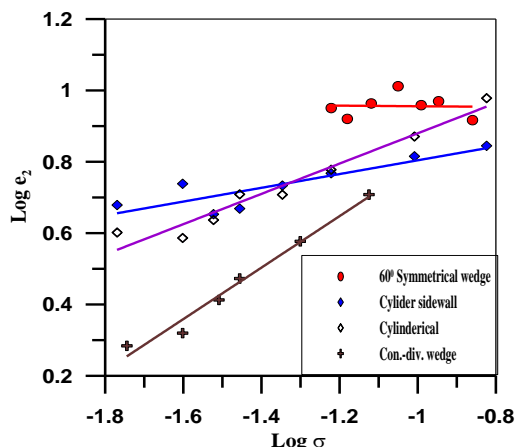
Fig.13. Variation of size exponent e_2 with cavitation number at various flow velocities for various sources.

Figure 10 indicates that the size exponent, e_1, appears to increase with flow velocity for both the 60^0 symmetrical wedge and circular cylinder with side-wall specimens. However a slight increase in e_1 is notice for both the con.-div. wedge with sidewall specimens and circular cylinder specimens.

From Figure 11, it can be seen that the value of the size exponent, e_2, decreases with increasing the flow velocity for all cavitation sources. Figure 12 illustrates that, for all cavitation sources (except the 60^0 symmetrical wedges), the size exponent, e_1, and increases with increasing cavitation number. However, in the case of the 60^0 symmetrical wedge source, the size exponent, e_1, decreases with cavitation number. The size exponent, e_2, is found to increase with cavitation number for all cavitation sources as indicated in Figure 13.

Figures 10 to 13 indicate that the size exponents (e_1 and e_2) may be approximated by exponential dependences of both flow velocity and cavitation number. From these Figures the exponential dependences (n_1, n_2, m_1, and m_2) were obtained and are presented in Table A3 (shown in appendix A) with the correlation coefficients.

As shown in Table A3 the magnitude of the exponents of both velocity and cavitation number (n_1, n_2, m_1, and m_2) for the size exponent's e_1 and e_2 vary widely over the different flow velocity and cavitation number ranges and to be dependent on the source shape and the erosion place. The reason for this wide variation in the exponents (n_1, n_2, m_1, and m_2) is not obvious.

It is evident that the present results are indicative of the complexity of the phenomenon of cavitation erosion. In addition, they reflect the general difficulty in scaling cavitation erosion with source size according to simple similarity laws. Thus further extensive experimental studies must be conducted to obtain true cavitation erosion size scale effects for various cavitation types at dynamically similar flows encountered in practice.

4. CONCLUSIONS

The following are the important conclusions which can be drawn from the reported extensive experimental investigation:

1. The results of the variation of weight loss rate with source size at either constant velocity and variable cavitation number or vice-versa indicated that the weight loss rate passes through a maximum as the source size increased. The maximum weight loss rate was found to occur at a blockage ratio of ≈ 0.5. Therefore, the range of blockage ratio nearer to 0.5 must be avoided to prevent serious damage and to increase the life of the cavitating equipment.

2. There was a power law relation between WLR and source size (i.e. $WLR \propto D^{e_1}$, $WLR \propto D^{e_2}$) .The size exponents varied widely from 1.88 to 5.1 ,(e_1), for blockage ratio up to ≈ 0.5 and from -1.93 to -11.3, (e_2), for blockage ratio larger than ≈ 0.5 depending on the flow conditions, geometry of the cavitation source and place of erosion.

3. The size exponents (e_1 and e_2) were varied exponential with the flow velocity and cavitation number. The magnitudes of flow velocity and cavitation number exponents were varied quite considerably depending on the cavitation source shape and place of erosion measurements. The size exponents varied widely from 1.88 to 5.1, (e_1), for blockage ratio up to 0.5 and from -1.93 to -11.3, (e_2), for blockage ratio larger than 0.5 depending on the flow conditions, geometry of the cavitation source and place of erosion.

4. The interesting feature of the present results is the fact that the flow conditions have a major effect on the value of the size exponent, i.e., there is no general size exponent for cavitation damage. Therefore the exponents of the order 1.7 to 8 reported in literatures cannot be regarded as a law for general application,

5. Further systematic investigations are necessary to provide some guidance for the hydraulic designers for the variations in size scale exponents.

REFERENCES

[1] Rao, P.V. and Buckley, D.H., "Cavitation Erosion Size Scale Effects", Wear, 96 (3), (1984), pp.239-253.

[2] Ramamurthy, A.S., Ranganath, Y.S. and Carballada, L.B., "Pressure and Source Size Effects on Cavitation Damage", Journal of Hydraulic Engineering, 110 (10), (1984), pp.1490-1494.

[3] Ramamurthy, A. S. and Bhaskaran, P., "Source Size and Velocity Effects on Cavitation Damage", Journal of Fluids Engineering, 97(3), (1975), pp. 384-386.

[4] Hammitt, F.G., "Cavitation Damage Scale Effects-State of Art Summarization", Journal of Hydraulic Research, 13(1), (1975), pp.1-17.

[5] Hammitt, F.G., "Cavitation and Multiphase Flow Phenomena", Mc Graw-Hill, (1980).

[6] Shalnev, K., Varga, J. and Sebestyén, G., "Scale-Effect Investigation of Cavitation Erosion Using the Energy Parameter", In Erosion by Cavitation or Impingement. ASTM International, (1967).

[7] Shalnev, K.K., Varga, I.I. and Sebestyen, D., " Investigation of the Scale Effects of Cavitation

Erosion", Philosophical Transactions of the Royal Society of London A: Mathematical, Physical and Engineering Sciences, 260(1110), (1966), pp.256-266.

[8] Malyshev, V. and Pylaev, N.I.K.O.L.A.I., "Influence of Hydro turbine Size on Cavitation Pitting Intensity", In Conference on Cavitation, Institution of Mechanical Engineers, London, Heriot Watt University, Edinburgh ,(1974), pp. 309-312.

[9] Thiruvengadam, A. and Preiser, H.S., "On Testing Materials for Cavitation Damage Resistance", No. TR-233-3, (1963), Hydronautics Inc Laurel MD.

[10] Thiruvengadam, A., "The Concept of Erosion Strength", In Erosion by cavitation or impingement, ASTM International, (1967).

[11] Stinebring, D.R., Holl, J.W. and Arndt, R.E., " Two Aspects of Cavitation Damage in the Incubation Zone: Scaling by Energy Considerations and Leading Edge Damage", Journal of Fluids Engineering, 102(4), (1980), pp.481-485.

[12] Rata, I.M., "Erosion de Cavitation—Mesure de l'erosion par jauges resistantes", In Societe Hydrotechnique de France, Symp. de Nice, (1960).

[13] Meier, W. and Grein, H., "Cavitation in Models and Prototypes of Storage Pumps and Pump Turbines", In Proc. IAHR Symp., Stockholm, International Association for Hydraulic Research, (1970).

[14] Schiele, O., Hergt, P. and Mollenkopf, G., "Some Views on the Different Cavitation Criteria of a Pump", In Proceeding of the 5th Conference on Fluid Machinery, (1975).

[15] Lashkov, A.S., "A Method for Predicting the Rates and Location of Points of Cavitation Induced Wear in Hydraulic Turbines", Fluid Mech.—Sov. Res, 6, (1977), pp.88-100.

[16] Hutton, S.P. and Guerrero, J.L., "The Damage Capacity of Some Cavitating Flows", In 5th Conference on Fluid Machinery, Vol. 1, (1975), pp. 427-438.

[17] Conn, A.F. and Mehta, G.D., "A Preliminary Evaluation of 3K SES Propulsor Erosion Damage Predictions", HYDRONAUTICS, Incorporated Technical Report, (1977), :7750-1.

[18] Mehta, G.D. and Conn, A.F., "A review of Cavitation Erosion Scaling Research", In Proc. 18th Am. Towing Tank Conf., Annapolis, MD, (1977), pp. 1-23..

[19] Hockworth, J.V., "On Erosion by Solid and Liquid Impact", Cambridge, Proc- 5th Conf., (1979).

[20] He, J.G. and Hammitt, F.G., "Velocity Exponent and Cavitation Number for Venturi Cavitation Erosion of 1100-O Aluminum and 1018 Carbon Steel", Wear, 80(1), (1982), pp.43-58.

[21] Varga, J.J., Sebestyen, G. and Fay, A., "Detection of Cavitation by Acoustic and Vibration-Measurement Methods", La houille blanche, (2), (1969), pp.137-150.

[22] Young, F. R., "Cavitation", (1989), McGraw-Hill, New York.

[23] Krieger, J. R. and Chahine, G. L., "Acoustic Signals of Underwater Explosions near Surfaces", The Journal of the Acoustical Society of America, 118(5), (2005), pp. 2961-2974.

[24] Chahine, G. L., "Experimental and Asymptotic Study of Non-spherical Bubble Collapse", Applied Scientific Research, 38(1), (1982), pp. 187-197.

[25] a) Blake, J. R., Taib, B. B. and Doherty, G., "Transient Cavities Near Boundaries", Part 1. Rigid Boundary, Journal of Fluid Mechanics, 170, (1986), pp.479-497.
 b) Blake, J. R., Taib, B. B., and Doherty, G., "Transient Cavities Near Boundaries", Part 2. Free Surface, Journal of Fluid Mechanics, 181, (1987), pp. 197-212.

[26] Zhang, S., Duncan, J. H. and Chahine, G. L., "The Final Stage of the Collapse of a Cavitation Bubble Near a Rigid Wall", Journal of Fluid Mechanics, 257, (1993), pp. 147-181.

[27] Jayaprakash, A., Hsiao, C. T. and Chahine, G., "Numerical and Experimental Study of the Interaction of a Spark-Generated Bubble and a Vertical Wall", Journal of Fluids Engineering, 134(3), (2012), pp. 031301.

[28] Best, J. P., "The Formation of Toroidal Bubbles Upon the Collapse of Transient Cavities", Journal of Fluid Mechanics, 251, (1993), pp. 79-107.

[29] Brujan, E. A., Keen, G. S., Vogel, A. and Blake, J. R., "The Final Stage of the Collapse of a Cavitation Bubble Close to a Rigid Boundary", Physics of Fluids (1994-present), 14(1), (2002), pp. 85-92.

[30] Hosien, M.A. and Selim, S. M., "Noise Produced By Cavitation From Various Cavitating Sources" Mansoura Engineering Journal, (MEJ), Vol. 40, Issue 4, (2015).

[31] Hosien, M.A. and Selim, S. M., "Acoustic Detection of Cavitation Inception", Journal of Applied Fluid Mechanics, Vol. 10, No. 1, (2017), pp. 31-40.

Appendix A

Table A1 Exponent (e) for size reported in literature.

Investigators	Device	Test conditions	e
Rao and Buckley [1]	Venturi and rotating disk	Overview and erosion data analysis (various devices)	1.7 to 4.9
Ramamurthy et al. [2]	Rotating disk	Two dimensional triangular prismatic used as cavitating sources	Critical size for max. erosion increases with cavitation number
Ramamurthy and Bhaskaran [3]	Rotating disk	Velocity, 39.5 m/s; cavitation number, σ = 0.196; circular cylinders inducer (During erosion).	3.3 to 4.9
Hammitt [4]	Hydro-turbines	Not available	4
Shalnev [6]	Venturi	Velocity, 12 m/s, circular cylinders, 24 and 48 nun diam. (During incubation period).	3
		During advanced stages of erosion	4
Shalnev [7]	Venturi	Same as above. (Using critical point erosion).	3
Malyshev and Pylaev [8]	Venturi similar to nozzles	Velocity, 36. 5 m/s and 0.628 MPa, source diameters, 1,2,4,6 and 8 mm, σ = 0.44 (Cavitation pitting)	3
Rata [12]	Schroter- Walcher	Velocity, 30-40 m/s (Zinc and brass plates)	8 to 8.4
Meier and Grein [13]	Pump and pump turbines	Complete operating range (cavitation intensity α (delivery head)^n) .	3
Schiele and MollenKopf [14]	Hydro-turbines	NPSH $_{pump}$ / NPSH $_{plant}$	3
Lashkor [15]	Hydrodynamic turbines	Erosion on blades and rotors of different materials	2
Hutton and Lobo Guerrero [16]	Venturi	Velocity 5-45 m/s (pitting)	2.2 to 3.5
Hackworth [19]	Models of ship propellers	Pitting	2.3

Table A2. Size exponents, e_1 and e_2 experimental results for various cavitation source configurations and test conditions.

Configuration shape	Erosion place		e₁ and e₂ and test conditions.															
60⁰ Symmetrical wedge	Sidewall erosion	σ & u	σ = 0.113								u = 37.6 [m/s]							
			42.5	40	37.6	35.31	33	30.2	28	24	0.06	0.066	0.076	0.089	0.102	0.113	0.138
		e_1	3.746	3.568	2.712	2.94	2.723	2.778	2.241	1.876	3.667	3.498	3.38	3.468	2.93	2.74	2.585
		r	0.9966	0.9876	0.986	0.985	0.933	0.934	0.953	0.977	o.870	0.934	0.944	0.981	0.951	0.986	0.938
		e_2	-3.822	-4.916	-6.07	-6.676	-6.77	-7.23	-10.15	-10.4	-8.43	-8.327	-9.2	-10.274	-9.12	-9.33	-8.26
		r	0.970	0.9517	0.876	0.879	0.923	0.992	0.966	1.0	0.919	0.867	0.743	0.774	0.936	0.876	0.9299
Circular cylinder	Sidewall erosion	σ & u	σ = 0.035								u= 37 [m/s]							
			40	37	34	31	28	24		0.017	0.025	0.03	0.035	0.045	0.06	0.098	0.15
		e_1	3.3	3.102	3.26	4.023	2.213	2.213		2.88	3.006	3.24	3.105	3.444	3.615	3.741	4.63
		r	0.967	0.984	0.955	0.998	0.979	0.952		0.502	0.991	0.986	0.984	0.981	0.965	0.969	0.966
		e_2	-3.2	-4.67	-5.24	-7.293	-10.49	-10.55		-4.78	-5.48	-4.502	-4.67	-5.45	-5.86	-6.54	-7
		r	0.98	0.961	0.924	0.993	0.991	0.992		0.923	0.992	0.992	0.961	0.986	0.988	0.991	0.999
	Cylindrical erosion	e_1	4.09	4	4.02	4.12	3.714	3.68		4	3.8	3.88	4	4.26	4.18	3.92	5.09
		r	o.992	0.992	0.985	0.991	0.988	0.979		0.971	0.978	0.984	0.991	0.994	0.951	0.953	0.974
		e_2	-3.45	-5.117	-5.01	-8.06	-10.23	-11.3		-4	-3.86	-4.34	-5.12	-5.1	-6	-7.43	-952
		r	0.999	0.944	0.96	0.984	0.971	0.993		0.979	0.943	0.992	0.944	0.992	0.962	0.981	0.942

Con.-div. wedge	Sidewall erosion	σ & u	σ = 0.035						u = 37 [m/s]					
			40	37	34	31	28	24	0.018	0.025	0.031	0.035	0.050	0.075
		e_1	3.13	3.012	3.07	2.855	2.92	2.876	2.014	2.11	2.312	3.012	3.65	5.086
		r	0.993	0.983	0.982	0.979	0.943	0.964	0.947	0.993	0.993	0.983	0.957	0.995
		e_2	-3.14	-2.97	-3.494	-3.81	-4.85	-5.89	-1.925	-2.09	-2.591	-2.972	-3.745	-5.103
		r	0.939	0.948	0.954	0.999	0.971	0.978	0.932	0.939	0.920	0.948	0.901	0.936

Table A3. Exponential dependences of both the flow velocity and cavitation number for source size exponents e_1 and e_2.

Source shape	Erosion place	$e_1 \approx u^{n_1}$	$e_1 \approx \sigma^{m_1}$	$e_2 \approx u^{n_2}$	$e_2 \approx \sigma^{m_2}$
		n_1	m_1	n_2	m_2
60^0 Symmetrical wedge	Sidewall erosion	1.11	-0.432	--1.66	-0.004
Circular cylinder	Sidewall erosion	0.851	0.2022	-2.43	0. 0.193
	Cylindrical erosion	0.215	0.090	-2.38	0.424
Con.-div. wedge	Sidewall erosion	0.162	0.692	-1.33	0.722